

# NONDETONATIVE EXPLOSIONS AND BURNING OF COMPOSITION-B EXPLOSIVE

Avi Birk, Patrick Baker, Douglas E Kooker, Robert Lieb, Steven Stegall  
Weapons and Materials Research Directorate/U.S. Army Research Laboratory  
Aberdeen Proving Ground, MD 21005-5066

John Delaney

U.S. Naval Explosive Ordnance Disposal Technology Division, Indian Head, MD 20640

This paper describes experiments towards establishing a predictive capability for nondetonative reactions in confined explosive systems. Composition-B was confined in steel tubes of various thicknesses and pressurized in separate experiments by self combustion and at various rates with a piston. Reactions were observed with high-speed film and embedded pressure gages. Many of the reactions possessed characteristic secondary ignitions away from the expected combustion surface or loading surface. These ignitions frequently start when the pressure is less than 1 kBar, and they play a major role in the reaction character. After secondary ignition, reaction violence was primarily driven by the strength of the confinement in a tradeoff between pressurization due to combustion and venting after confinement has failed. The former is directly determined by the burning rate of the Comp-B and the surface area available for burning. Strand burner, closed bomb, and vented chamber experiments were conducted to examine the burning behavior and regression rate. The process seems to be reproducible up to pressures of ~100 MPa. At greater pressures, the pressurization rates indicate that Comp-B may be rapidly deconsolidating. In the vented chamber, Comp-B samples were quenched at ~35 to 125 MPa. Scanning electron microscopy of the quenched surfaces showed pits consistent with a mechanism whereby RDX particles are dislodged from the surface during the burning process. These results, when examined with results from other studies, offer an opportunity for better understanding the explosion response for Comp-B and other melt cast explosives.

## INTRODUCTION

We have been studying the nondetonative response of confined explosives to impact. Previously<sup>1,2</sup> we identified six possible reaction types following impact: (1) prompt detonation, (2) delayed detonation, (3) violent explosion, (4) mild explosion, (5) burn, and (6) quench/no-reaction. Our goal is to understand what determines the reaction type and to develop a predictive capability. In many impact scenarios, the desired reaction type is mild explosion. Experience has shown that heavily confined Comp-B (59.5% RDX; 39.5% TNT, 1% wax) frequently undergoes violent explosions. This results from Comp-B's brittleness and the rapid burning of its RDX filler. TNT on the other hand, normally generates mild explosions when confined charges are impacted. Previous efforts have focused on the mechanical response of TNT and Comp-B,<sup>3</sup> creating a model for the burning of confined explosives with venting,<sup>4</sup> microscopic studies of TNT and Comp-B burning behavior,<sup>5</sup> experiments to elucidate confined nondetonative reaction,<sup>6,7,8,9</sup> and effective burning rate studies of explosives<sup>10</sup>. This paper describes nondetonative experiments and a variety of combustion studies on Comp-B. Rates and mechanisms identified in the latter shed considerable

insight on the qualitative and quantitative reaction growth observed in confined Comp-B.

## NONDETONATIVE REACTION GROWTH

Three types of reaction growth experiments have been conducted on Comp-B.<sup>7,8</sup> In all three, the explosive was cast in 1026 series steel tubes of various thicknesses. A schematic of the experiments is shown in Figure 1. In all three, the tube internal diameter was 50.8-mm, and the explosive column is 0.61 m long. Tube thickness was varied to study the effect of confinement.

The ignition method varied between configurations. In **A**, the explosive was ignited with a BKNO<sub>3</sub> ignition mix contained in a small cavity. In **B**, a piston rapidly compressed the Comp-B. The piston was driven with smokeless pistol powder in an adjacent driving section. Pressurization rate and peak pressure were varied. In configuration **C**, the explosive was ignited directly using a small amount of smokeless powder in an adjacent ullage section. In principle, the additional ullage between **C** and **A** should slow the rate of pressurization. Furthermore, configuration **C** provided a geometry and pressurization rate more conducive to

simulation. Instrumentation on these tests included embedded carbon resistor gages<sup>11</sup> as shown in Figure 1, high-speed photography, and piezoelectric pressure gages in the ignition section of configuration C. All resistor gage pressures reported here were reduced using a common calibration given in reference [9]. Additional details can be found in references [7] and [8]. The primary results and conclusions are summarized here.

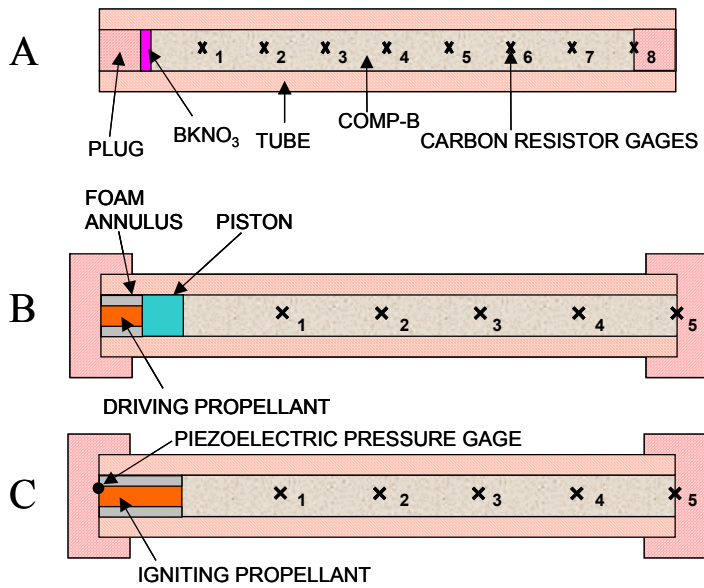


**FIGURE 1. THE TUBE EXPERIMENT.**

DIRECT IGNITION : CONFIGURATION A

In configuration A, tube thicknesses of 3.18, 6.35, 12.7 and 25.4 mm were used to conduct ten tests. The explosive was ignited at one end and reaction behavior was observed. The explosive yield increased with tube thickness, and the size of the resulting fragments decreased. The pressure gages recorded waves emanating from the combustion region and propagating axially in the Comp-B.

The most striking artifact of these tests was a frequent secondary reaction that occurred some distance from the designed burning surface. Figure 2 illustrates such a reaction in a 6.35-mm-thick tube. Time has been adjusted to account for ignition delay. The top of Figure 2 shows a rise in the pressure at Gage 2 before Gages 1 or 3; this indicates a rapid secondary reaction some distance away from the initial burning surface, in this case ~150 mm. The bottom of Figure 2 shows a high-speed film image of this secondary reaction at a frame spacing of ~29 μs. The film record supports the gage indication that a violent reaction breaks out in the vicinity of Gage 2.

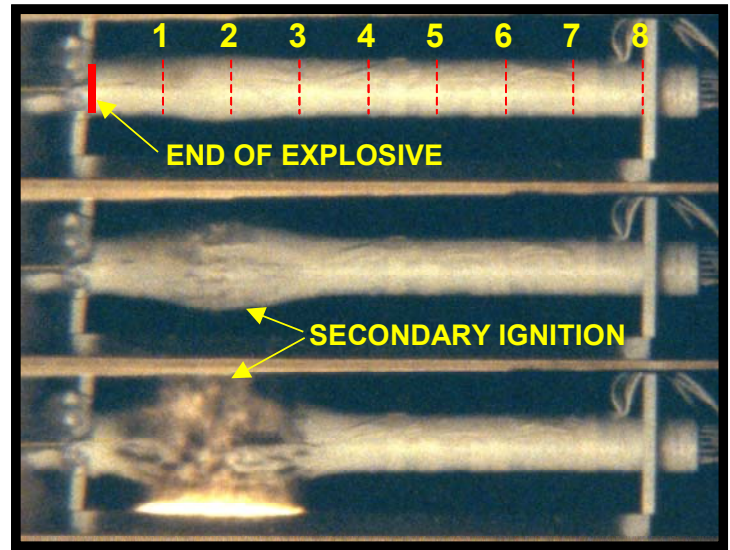
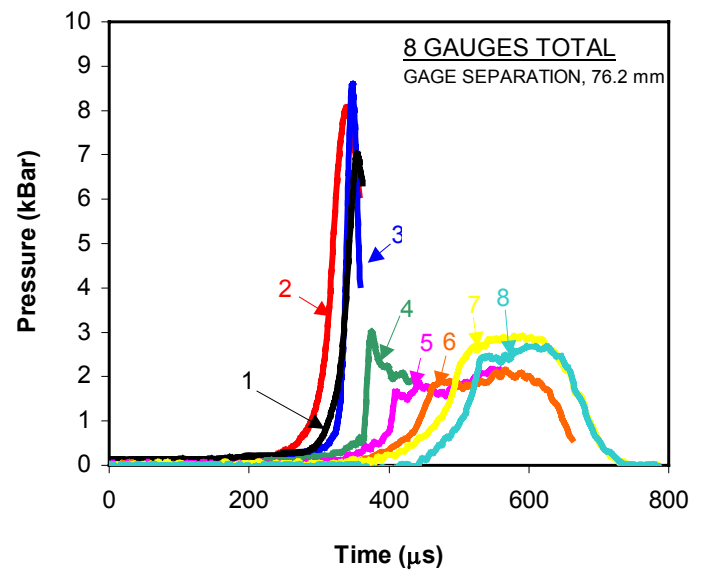


**FIGURE 2. PRESSURE AND PHOTOGRAPHIC RECORDS FROM SELF-IGNITED COMP-B IN 6.35-MM-THICK STEEL TUBE.**

Confinement strength in the combustion region determined whether the pressure increased or decreased. For thinner tubes, the reaction quenched and the pressure was decreased by release waves; for thicker tubes, the reaction grew and drove the propagating wave towards a shock. In Figure 2, the pressure waves from the secondary reaction then propagate axially in both directions, as evidenced by Gages 1 and 3. The prompt fracturing of the tube caused release waves to decrease the pressure. By the time it reaches Gage 4, it has formed a shock, but its magnitude has decreased. The wave then propagates at a relatively constant value toward Gage 8. Because the pressure is low and release waves are influential, the shock becomes a ramped compression wave. The propagation speed of these waves is nominally the sound speed of the explosive.

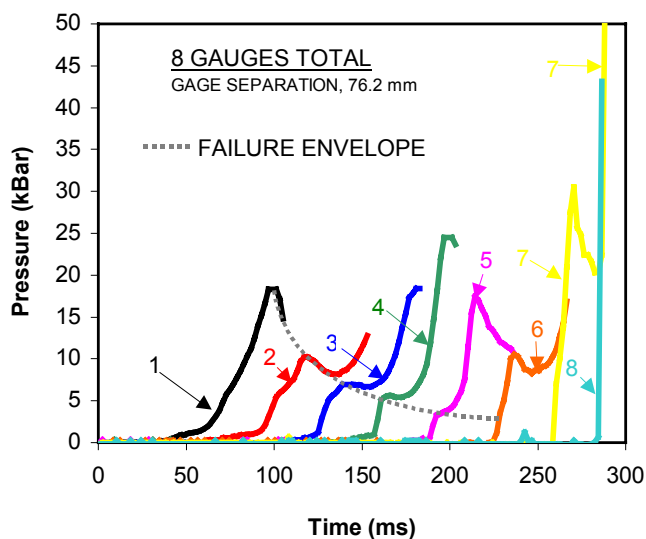


**FIGURE 3. PRESSURE HISTORY FROM COMP-B IGNITED IN A 25.4-MM-THICK TUBE.**

For thicker tubes, which resulted in stronger reactions, the pressure waves showed significant steepening and shocks began to form. Figure 3 shows a typical pressure response from configuration **A** with a 25.4-mm-thick tube. The pressure is much higher than for a thinner tube, and the compression wave forms a shock. The shapes of these pressure records seem to indicate a release wave associated with tube failure that is followed by a strong reaction wave driving a further pressure increase. The dash line in Figure 3 is meant to indicate the path of the initial release wave in the P-t space. The strong compression, due to the subsequent reaction, overtakes this release wave between Gages 6 and 7.

#### PISTON IGNITION : CONFIGURATION B

The experiments with configuration **A** did not indicate the origin of the secondary reaction in Comp-B. Mechanical initiation and convective burning were two possible sources. Thus, experiments were conducted with configuration **B**, where a piston drove an initially inert pressure wave into the Comp-B. The type and quantity of smokeless powder in the driving section were chosen to vary peak pressure and pressurization rate. These values were calculated with the XKTC code.<sup>12</sup> 22 tests were conducted with pistons. 12 tests used 25.4-mm-thick tubes, and 10 used 6.35-mm-thick tubes.

The general sequence of events for these tests is that, first, the propellant is ignited by the squib and the pressure rises to push on the piston. This sends a pressure wave axially down the tube at the sound speed of the explosive. The initial shape of this compression wave is dictated by the driving pressure history, but

this can be augmented by reacting Comp-B or decremented by release waves as the tube yields and fractures. In most experiments, at some point the Comp-B ignites.

Pistons were recovered from several of the milder reactions and did not show evidence of high-pressure gas blow-by. However, ignition from the driving propellant gases cannot be entirely ruled out, particularly after the tube yields. Nonetheless, clear evidence of mechanical initiation was shown for some tests; it is believed to be the primary initiation mechanism.

25.4-mm-Thick Tubes: All twelve 25.4-mm-thick tubes resulted in violent explosions, which were less than detonations but had ~100% explosive yield. Thus, the reaction violence was independent of the loading rate that led to the reaction. It is possible that detonation occurs in a pulverized explosive after the tubes significantly expand, but the resistor gages are destroyed during the event, so it is difficult to tell. At the peak loading of 4.56 kBar in 205  $\mu$ s, the pressure rise time is less than the compression wave travel time over the length of explosive and back (~400  $\mu$ s). At the lowest loading rate (2.34 kBar in 4900  $\mu$ s), the loading occurs over more than 10 wave cycle times in the explosive.

Comparison of gage records for three loading rates provides insight into this event. Figure 4 shows pressure records for a high-pressure high-loading-rate (4a, 4.56 kBar in 205  $\mu$ s), low-pressure medium-loading-rate (4b, 1.27 kBar in 655  $\mu$ s), and high-pressure low-loading-rate (4c, 4.05 kBar in 3300  $\mu$ s). For the highest rate, the reaction is rapid and during the initial pressurization. Failure of the tube is believed to occur in the 4-kBar range because a characteristic rollover of the pressure curve seemed to occur for most 25.4-mm-thick tube experiments. After this, a release wave reduces the pressure. However, the pressure then starts to increase again because it is supported by reaction in the fragmented Comp-B.

Based on the gage behavior in Figure 4a, we believe a secondary ignition occurred at some location down the tube. This idea is supported by, first, Gage 3 detecting a secondary pressure rise without a preceding rise in Gage 2, and second, by the time between the 5–9 kBar regions of Gages 1 and 3 being much less than the time between the 1–3 kBar regions. The latter is commensurate with the sound speed, whereas the

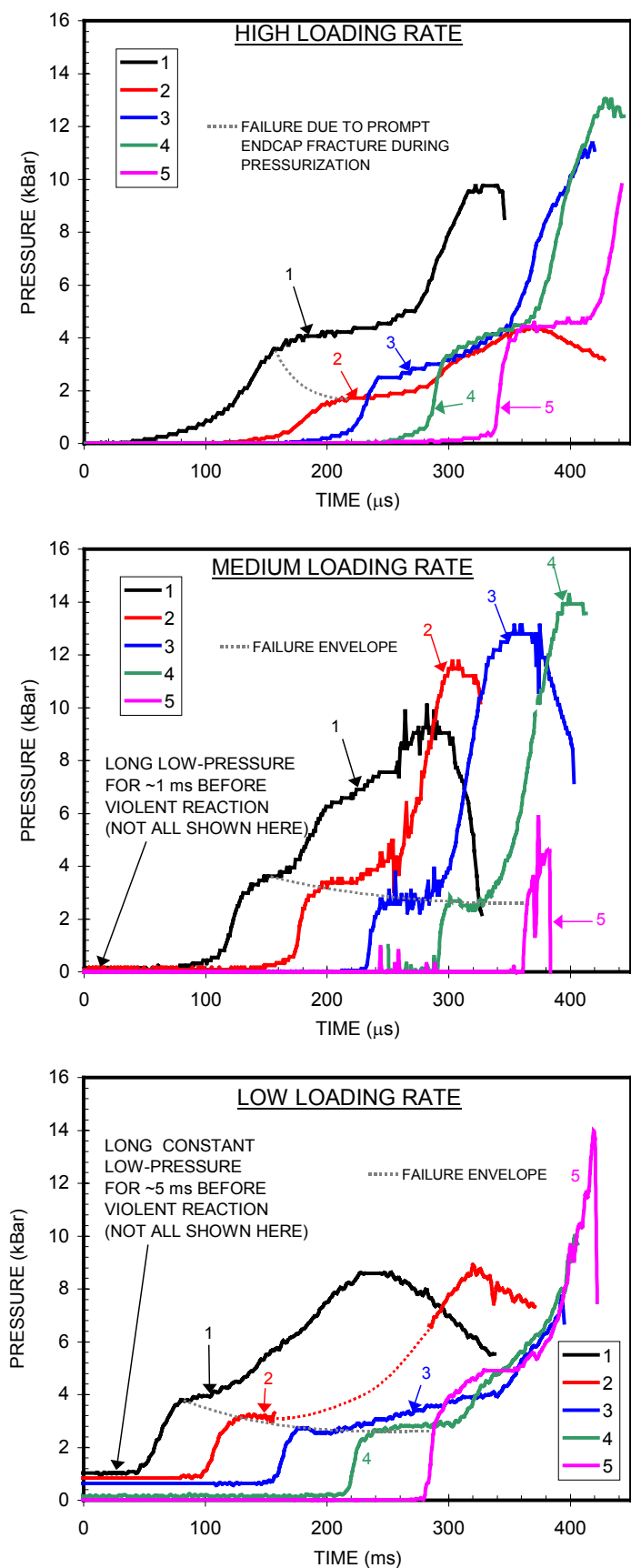


**FIGURE 4. PRESSURE HISTORY IN A 25.4-MM-THICK TUBE PRESSURIZED WITH A PISTON AT THREE DIFFERENT RATES.**

former is too short. Thus, a secondary reaction is believed to occur between Gages 3 and 4.

Figures 4b and 4c show a long constant low-pressure region before ignition. Thus, wave motion in these tests does not appear responsible for ignition. After ignition, the sequencing pressure records (1–5) indicate that ignition occurred between the piston and the first carbon gage. When ignition does occur, the pressure rolls over at a pressure associated with tube failure. In Figure 4c, the constant pressure lasted for ~5 ms before ignition occurred, and the value of this pressure decreased with distance away from the piston. This indicates that significant shear force exists between the Comp-B and the tube wall, thus decreasing the axial load taken up by the explosive as the distance gets farther away from the piston. Indeed, near the last gage, very little load is actually on the far end cap before ignition. This process opens up the possibility of sudden mechanical failure and friction between the explosive and the tube wall leading to a mechanical mechanism of ignition.

An exaggerated example of mechanical initiation is shown in Figure 5. In this test (2.75 kBar in 325  $\mu$ s), a compression wave propagated the length of the explosive and reflected back toward the piston. At the center of the tube near Gage 2, the tube's boundary was disturbed by a metal wedge between the tube and a witness plate. After the wave passed by this perturbed region, there was an ignition between Gages 1 and 2. Based on the arrival times of the pressure waves at the gages, the reaction is estimated to begin about 30–40 mm on the Gage 1 side of Gage 2 (~25–33% towards Gage 1 from Gage 2). Two observations can be made from this result. First, mechanical initiation is possible and likely in these types of tests, and second, once the reaction begins the pressure rises extremely rapidly as shown by the Gage 2 record.

**6.35-mm-Thick Tubes:** The reactions from the thin tubes varied from no reaction to delayed detonation, and there was a definite effect of driving pressure on several experiments. For the fastest loading rate (2.75 kBar in 325  $\mu$ s), a delayed detonation occurred repeatedly in two tests. The loading rates in these tests are the same as in the test in Figure 5 for the 25.4-mm-thick tube. Figure 6 shows the pressure wave and resulting detonation. Comparing Figures 5 and 6, we observe that the pressure leveled off in the thicker tube while the wave was propagating the length of the tube and being reflected back, but in the thinner tube the pressure on Gage 1 only levels off for a short time and then begins to rise. This is believed to be due to the reaction of the explosive. However, as the reaction is quenched by release of confinement (photographs show

the tube is splitting), the pressure drops as a release wave propagates down the tube. About 200  $\mu\text{s}$  after the pressure drops to zero, the explosive detonates. We believe the detonation is due to recompression of Comp-B damaged during the release process. The sequencing of the gage records indicates that the detonation began between the piston and Gage 1.

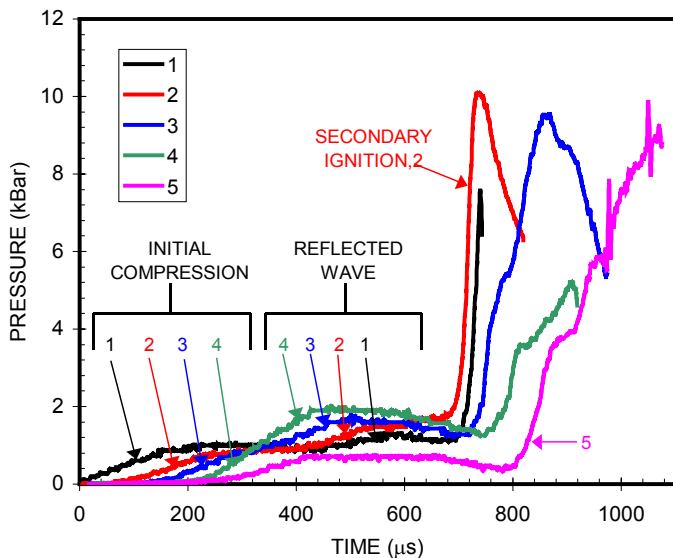
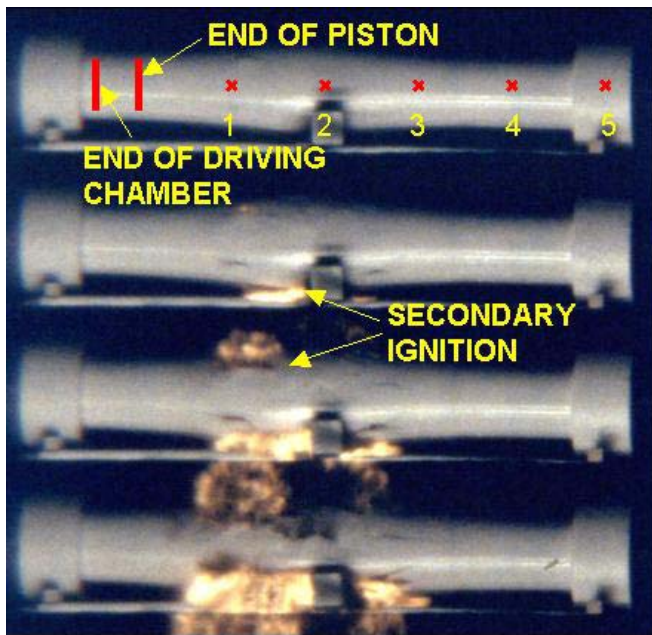


**FIGURE 5. DIRECT EVIDENCE OF A MECHANICALLY CREATED SECONDARY REACTION IN A 25.4-MM-THICK TUBE.**

Other than the detonations, the remaining tests with the 6.35-mm-thick tubes resulted in very mild reactions or no reactions. In nearly all cases, large quantities of unreacted explosive remained. One test with a long loading rate (4.05 kBar, 3300  $\mu\text{s}$ ) resulted in a mild explosion. However, with this thin wall and the long pressurization rate, the effectiveness of the piston in blocking propellant gases is suspect.

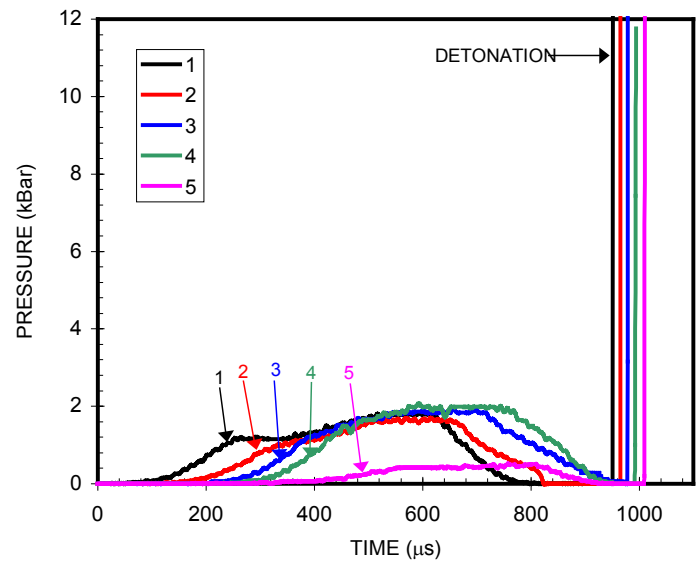


**FIGURE 6. PRESSURE WAVE FROM A DETONATION TEST IN A 6.35-MM-THICK TUBE.**

### CONFIGURATION C: NO PISTON

Two tests were run without pistons to reexamine intentional Comp-B ignition and provide some data for comparison with a modeling effort.<sup>4</sup> In these tests, a small amount of smokeless Bullseye<sup>TM</sup> powder in a 101.6-mm combustion chamber was used to ignite the Comp-B. A PCB109 piezoelectric pressure gage was placed in the end cap next to the combustion chamber to give a more precise measure of chamber pressure. Pressure from the igniting propellant stabilized at  $\sim 0.144$  for 5 ms and 0.103 kBar for 10 ms for the 6.35-mm tube and 25.4-mm-thick tubes respectively. Then a violent reaction occurred, and the pressure rapidly increased. The chamber pressure histories are shown in Figure 7.

A rapid pressure rise from the burning Comp-B is expected; however, it will be shown later that this rise is much faster than predicted assuming that the Comp-B column burns cigarette-like based on the limited burning rate information available. A witness plate under the 25.4-mm-thick tube implied that somehow the reaction may have caused Comp-B to be moved into the combustion chamber where it perhaps underwent some type of XDT event. Interestingly, however, the detonation reaction did not propagate down the remainder of the tube. This behavior is consistent with a secondary reaction within the Comp-B ejecting material violently back into the combustion chamber where it is recompressed and detonates; the lack of contiguous explosive then prevents this detonation from propagating to the remainder of the charge. The combustion studies shed some light onto this possibility.

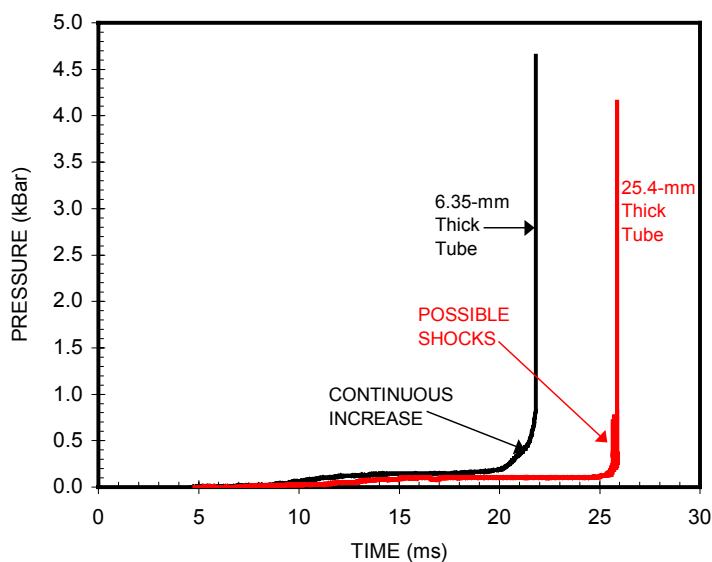


**FIGURE 7. PRESSURE IN COMBUSTION CHAMBER FROM CONFIGURATION-C TESTS.**

### COMP-B COMBUSTION STUDIES

Pressurization within the confinement is directly determined by the regression rate (RR) of the Comp-B and the surface area available for burning. The RR will be interpreted as an effective rate of surface regression, and not necessarily as the linear burning rate often associated with a layer-by-layer combustion process exhibited by common rocket and gun propellants. Complementing the tube experiments, strand-burner, closed-bomb, and interrupted/vented closed-bomb (referred to in the manuscript as the vented-chamber) experiments were conducted to examine the regression behavior and rate of Comp-B. The objectives are to, a) establish if the regression rate of Comp-B at 3–100 MPa can be formulated reliably as  $a \cdot P^n$ , b) conduct morphological study of quenched samples obtained at 40–100 MPa, and c) find out if Comp-B fails mechanically below 100 MPa as it self-pressurizes during combustion.

### COMBUSTION INSTRUMENTATION

The strand burner used by Miller and Vanderhoff<sup>13</sup> was employed for measuring the regression rate of TNT, Tritonal, and Comp-B in the range of 3–9 MPa in a constant-pressure nitrogen environment. The nominal strands, referred to here as free strands, were cylindrical, 6.4-mm in diameter and 32-mm in length. Other strands were cast in glass tubes of 6-mm inside diameter, 8.3-mm outside diameter and 30-mm length. The strands were ignited using hot wires and regression

rates were video-analyzed.

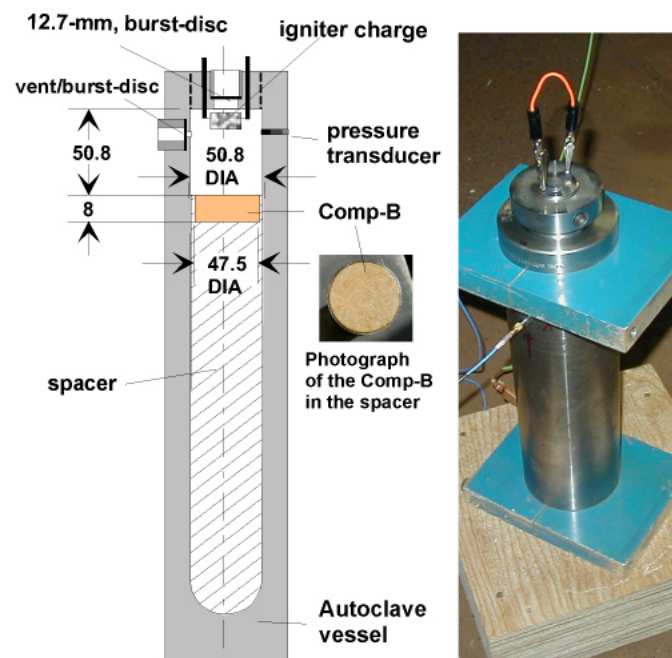


**FIGURE 8. VENTED-CHAMBER USED FOR INTERRUPTED BURNING TESTS (DIM. IN MM).**

For pressures above 9 MPa, a modified Autoclave vessel shown in Figure 8 was used as the vented-chamber. The vessel, rated at 210 MPa, has an inside diameter of 50.8 mm and an outside diameter of 102 mm. The Comp-B, with a shape resembling a hockey puck, was cast in a separate mold and polished to fit snugly into a recess in the top of a spacer inside the vessel as shown in the left side of Figure 8. The bottom and the curved sides of the Comp-B were coated with silicon grease to inhibit these surfaces from reacting. The configuration thus resembled an end-burning cylindrical cavity that is similar to the tube-without-piston experiment. The size of the cavity and the Comp-B were designed so that even in the absence of venting, the maximum pressure would not exceed the rated pressure of the Autoclave chamber. As shown in Figure 8, the Comp-B dimensions were, 47.5-DIA \* 8 mm, and the cavity dimensions were 50.8-DIA \* 50.8 mm. The Comp-B was ignited by pressurizing the cavity with hot gas from 0.7 g or 1 g of Bullseye<sup>TM</sup> powder activated with an electric match. A burst disc at the top of the cavity provided for rapid depressurization of the cavity and interruption of the burning of the Comp-B. Another burst disc on a side vent (1.5 or 2-mm diameter orifice) with a lower burst pressure than the top burst disc was used to modify the pressure rise rate, extending the time it would take to reach the bursting pressure of the top disc and hence providing deeper regression of the Comp-B.

Additional information was obtained from closed-bomb runs in a conventional 207-cc closed bomb. The bomb was loaded at  $\sim 0.2$  g/cc with solid cylindrical Comp-B grains 0.64-cm long and 0.64-cm in diameter.

### COMP-B REGRESSION RATE RESULTS

The combined results from strand-burner, closed-bomb, and the vented-chamber are plotted in Figure 9.

**Conventional Closed Bomb Results:** Comp-B regression rates (RR) were obtained from six tests. The RRs deduced from the closed bomb are repeatable up to the 90 MPa level. These RRs exhibit a distinct break at 23 MPa and a less distinct break at 91 MPa. (See Table 1.) Accordingly, RR laws in the form of  $RR = a \cdot P^n$  were fitted to three pressure ranges that border these breaks. The lower range is not considered reliable because a) it is affected by ignition process and heat losses and b) the explosive regressed only a fraction of a millimeter (by the time 21 MPa was obtained), and the regression may be affected by irregularities in material formulation near the grain surface.

**Strand Burner Results:** Below 1 MPa, there was no visible flame. At all pressures, the burning surface was not flat. The regression rate fluctuated below 5 MPa. The flame was very bright and unusually extended. Frequent dark streaking in the flame indicated ejection of material from the burning surface. Interestingly, a free strand of Tritonal (80% TNT, 20% aluminum), although generating considerable amount of soot, had a flame that in general appearance and dynamics resembled the Comp-B flames. The strands confined in glass tubes burned with a flatter surface and regressed at a much slower rate than the free strands. In the TNT glass-confined strands, a dark front seemed to proceed down the tube, almost obscuring the flame. The Comp-B-containing glass tubes, while sooty, remained intact after the burning. In the case of the TNT and Tritonal, the glass tubes were cracking a few millimeters above the burning surface and were filled with porous soot. In the pressure range tested (3–9 MPa), the strand regression rate could be formulated as  $RR = a \cdot P^n$ . As shown in Figure 9, the free-strand regression rate is higher than the closed-bomb rate even if extrapolated to higher pressures. Even the glass-confined strands regression rate, if extrapolated, intercepts the closed bomb data only above 50 MPa. The Tritonal RR (in glass tubes) was almost identical to that of the TNT. The TNT's RR is within the range found in Kondrikov et al<sup>14</sup> so we surmise that the data from the glass strands for all of the explosive tested are real.

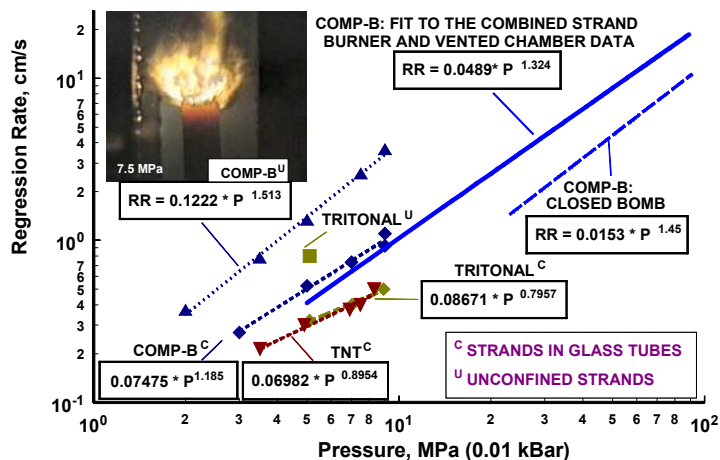


**FIGURE 9. REGRESSION RATES OF COMP-B, TNT AND TRITONAL. FREE STRANDS REGRESSED MUCH FASTER THAN STRANDS CONFINED IN GLASS TUBES.**

**Vented Chamber Results:** The tests are divided into three groups A, B, and C categorized by the amount of igniter used and surfaces ignited. In Groups A and B, 0.7-g Bullseye powder was used for ignition; 1 g was used in Group C. In Group A, the Comp-B burned ideally in the sense that only the top surface burned. In groups B and C, the circumferential or side surface reacted. Figure 10 depicts a typical pressure trace and examples of extinguished Comp-B recovered from the tests. 13 tests were conducted, (2 in Group A, 6 in B, and 5 in C). Quenching pressures were from 35–125 MPa. Note the significant amount of side burning, an indication that the flame propagated down the charge sides soon after ignition despite the snug contact of the charge with the metal. In all cases, the bottom surface did not react (the silicon grease effectively inhibited it). In those cases where the combustion was interrupted above 100 MPa, the recovered samples were found broken into large pieces.

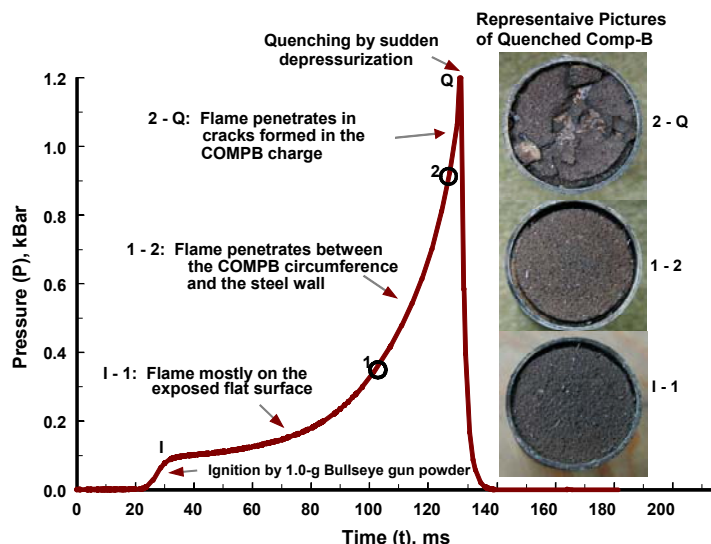


**FIGURE 10. TYPICAL RESULTS FROM THE VENTED-CHAMBER EXPERIMENT.**

The fractured surfaces were burned, an indication that the charges broke during combustion and not because of rapid depressurization. In those tests that exhibited unusually high early pressure rise rates, the Comp-B charges were found broken, an indication that the charges cracked at relatively low pressures. Early cracking of the charge occurred mostly with the stronger igniter, i.e., in Group-C tests. Because the grease coating always inhibited the bottom surfaces from burning, the regressions are attributed to top surfaces and are simply the difference between the thickness of the original Comp-B sample and the thickness of the extinguished sample. For each sample, multiple regression measurement were made and averaged. The top surfaces were found to regress uniformly with variation of less than 0.1 mm across. The regressions ranged between 1.3 and 3.6 mm. The depressurizations were much steeper than the pressurization, effectively extinguishing the burning instantly. The use of side venting was restricted to few tests because the side orifices (made of high-strength stainless steel) eroded severely.

### ESTABLISHING THE REGRESSION RATE

The RR law from the closed-bomb is deduced using a standard closed-bomb data reduction code. Establishing a regression rate law from the strand-burner regression rate data measurement is trivial. Establishing the RR law from the vented-chamber is done as follows. If the RR can be formulated as  $RR = a \cdot P^n$ , then 'a' and 'n' can be deduced in a manner shown in Figure 11.

If  $D_A$  and  $D_B$  are the regressions at points A and B, the RR parameters 'a' and 'n' are found from the iterative solution of

$$a \cdot \int_D^A P^n \cdot dt = D_A$$

$$a \cdot \int_D^B P^n \cdot dt = D_B$$

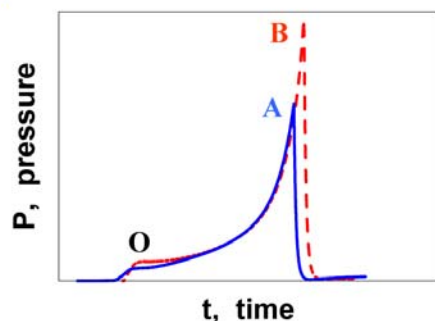


**FIGURE 11. METHOD OF FINDING THE REGRESSION RATE LAW.**

If the regression cannot be formulated as described then no solutions are obtained or the solution is not real. If the pressure traces of the pair of tests overlap and a solution is obtained, then the RR parameters so

found apply to the pressure range between the extinguishing pressures (the contribution from the lower pressures effectively cancel out). If the RR parameters are indeed constant over the entire range of all the tests then all combinations of pairs of tests should yield the same RR parameters regardless of their pressure profiles. The ideal tests for this analysis are tests that have overlapping pressure-time histories and large regressions that differ significantly from each other. We found that most test-pair combinations from Groups A and B yielded RR parameters while only few test-pair combinations from Group C alone, or Group C against Groups A and B, yielded the parameters. We suspect that the stronger igniter used in Group-C caused irregular regression and that skewed the analysis.

The Comp-B regression-rate laws found here from the various experimental techniques are summarized in Table 1. We suggest using the best fit from the strand-burner and the vented-chamber.

**TABLE 1. COMP-B REGRESSION RATE LAW.**

Experiment	Regression Rate Law $RR(\text{cm/s}) = a \cdot P(\text{MPa})^n$
Strand Burner (confined strands)	$a=0.07475$ $n=1.185$ $3 < P < 9$
Closed Bomb	$a=0.0153$ $n=1.45$ $23 < P < 91$ $a=0.00033$ $n=2.3$ $91 < P < 150$
Vented Chamber	$a=0.048$ $n=1.25$ $P \sim 60$ $a=0.025$ $n=1.52$ $P \sim 75$ $a=0.0031$ $n=2.0$ $P \sim 85$
Best Fit to the Strand Burner and Vented Chamber	$a=0.0489$ $n=1.324$ $5 < P < 90$

### MORPHOLOGICAL STUDIES OF QUENCHED COMP-B

All extinguished samples from the vented-chamber were analyzed using scanning electron microscopy (SEM). (See Lieb and Baker<sup>15</sup> regarding sample preparation and methodology.) Unlike Lieb and Baker<sup>15</sup>, the burning surfaces of all the samples regressed well beyond the first layer of RDX particles and thus are more representative of the in-depth process. The samples were cold-fractured to expose their interiors. Typical micrographs are depicted in Figure 12. The burnt surfaces appear white, the TNT

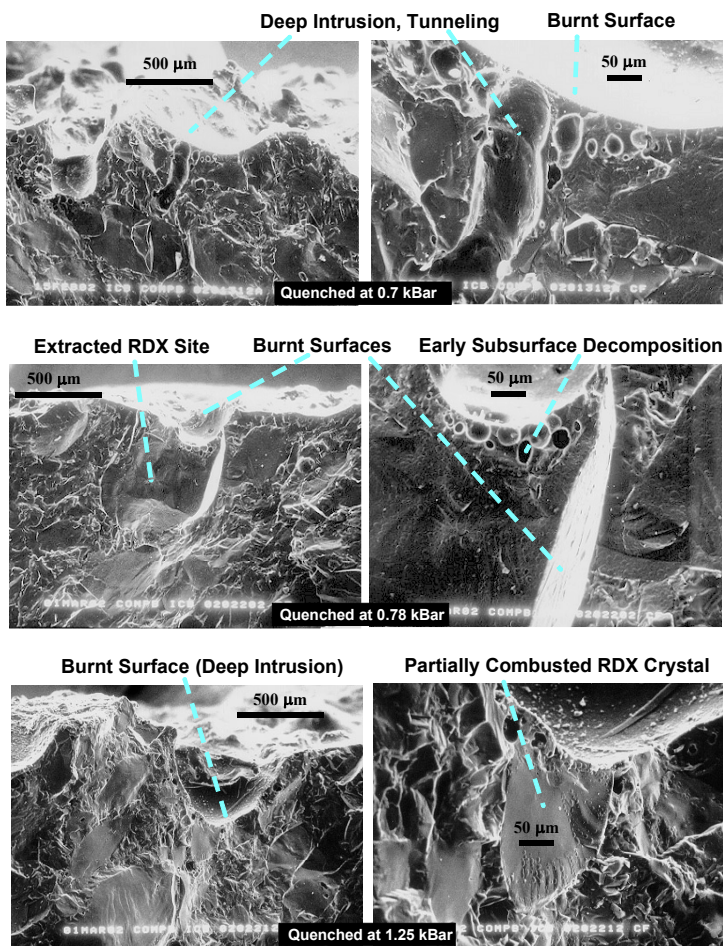


**FIGURE 12. SEM ANALYSIS OF THE INTERIOR OF THE EXTINGUISHED SPECIMENS.**

matrix appears “cobwebbed”, and the RDX particles appear as smooth areas with distinct boundaries. There are no voids in the virgin materials except occasionally in the largest RDX particles. The cobweb in the TNT indicates boundaries between TNT crystals. The exterior burning surface was cratered and had roughness on the order of 0.5 mm. Samples that were extinguished at higher pressure exhibited on the average smoother surface but no obvious trends could be deciphered. The present morphological findings do not differ from those found by Lieb and Baker.<sup>15</sup> It appears that there are subsurface decomposition zones within 100 μm underneath the reacting surface (see middle picture in Figure 12). It is not clear if these are due to reactions of very small RDX particles or decomposition occurring in the TNT matrix. Tunneling (shown in the top picture of Figure 12) is similar to what was found by Lieb and Baker<sup>15</sup> for extinguished samples of pure TNT. They speculated that the tunneling and subsurface decomposition zones provide a network of interconnecting passageways for the exterior combustion gas to ignite large subsurface RDX particles. The ignited RDX particles then burn rapidly, break loose from the TNT matrix, and thrust adjoining TNT material into the flame. This process

shows morphologically as deep intrusions (top picture) and extracted RDX sites (mid picture). As pressures get higher, the newly exposed surfaces in the extracted RDX sites re-ignite more rapidly and the regression rate accelerates. The bottom picture in Figure 12, taken for a sample extinguished at 125 MPa, shows a partially combusted RDX. No partially combusted RDX particles were found at lower pressures. Perhaps at higher pressures, the regression rate is limited by the burn rate of RDX particles (unless mechanical fracturing starts to dominate the regression mechanism).

## DISCUSSION AND CONCLUSIONS

The tube tests provide insight into nondetonative reactions of confined explosives. In many tests, compression waves were observed to travel through the charge with the approximate sound speed of the explosive. The strongest waves were seen to steepen into a ramp wave followed by a shock. Failure of the confinement was also seen to emanate release waves that travel behind the main compression wave and cause it to weaken. Secondary reaction observed in some of the tube tests can occur by several possible mechanisms. The piston tests showed cases of mechanically initiated secondary reactions. However, an analysis of the configuration C test in the context of the vented chamber results indicates that convective burning is a possible mechanism for secondary reaction. Using the best-fit regression rate from Table 1, we simulated configuration C test on the 6.35-mm thickness tube from Figure 7 using the code developed by Birk et al.<sup>4</sup> The results, shown in Figure 13, indicate that at 15 MPa, a ten-fold increase in effective regression rate or more likely burning area should have occurred. Such would be the case had the flame penetrated along the tube wall, as in Figure 10.

With respect to deflagration of Comp-B, the present observations seem to be consistent with the Comp-B regression mechanism proposed by Lieb and Baker.<sup>15</sup> This is based not only on the morphological studies of extinguished Comp-B but also on the peculiar disparity of RR observed in confined and non-confined strands. The present study found that un-confined Comp-B strands regress much faster than confined (in glass tube) strands. A similar effect was found with Tritonal that is composed mostly of TNT and does not contain reactive particles. Furthermore, cast Comp-B grains confined in a closed bomb exhibit a slower regression rate than unconfined strands of Comp-B. Apparently, in the absence of side confinement, subsurface tunneling into the TNT matrix expands and forms cracks that split and loosen the material. In a closed-

bomb environment, the grains, while not confined, burn on all surfaces; perhaps, the thrust reaction on the burning surface stabilizes the material.

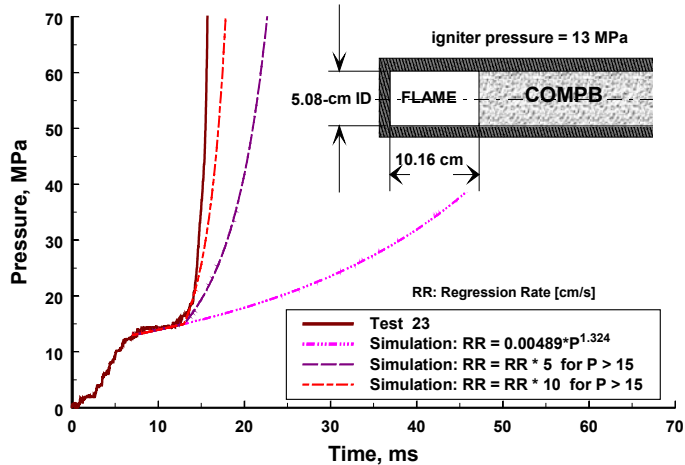


**FIGURE 13. SIMULATION OF TEST 23 INDICATES A SUDDEN INCREASE IN BURNING AREA.**

We suppose that the regression rate of Comp-B is influenced by the particle size distribution of the RDX in the TNT matrix. The regression mechanism involves injection of particulate material (TNT and RDX) into the flame. Both the closed-bomb analysis and the present study make us suspect that the Comp-B charge fails mechanically around 0.1 kBar, perhaps because of the absolute pressure level or the pressurization rate at that level. This may follow from the fact that Comp-B is very brittle and is susceptible to mechanical failure at low stress levels<sup>3</sup>. Above 0.1 kBar, all our observations to date suggest a Comp-B combustion process dependent on failing structural integrity and therefore nearly impossible to predict.

## REFERENCES

1. Baker, P.J. and Delaney, J.E. "Impact Initiated Detonative and Nondetonative Reactions in Confined Tritonal, Composition H-6, and PBXN-109," Eleventh Symposium (International) on Detonation, pp. 525-532.
2. Baker, P. J., S. Stegall, A. Canami, W. Slack and W. Boyd Jr. "The Effect of Case Strength, Path Length, and Main Explosive Charge Type on the Performance of Three Main Charge Disrupter Candidates," ARL-TR 2193, U.S. Army Research Laboratory, Aberdeen Proving Ground, MD, 2000.
3. Lieb, R.J., Starkenberg, J., Lawrence, W., and Baker, P.J. "Mechanical Damage and Combustion of TNT and Composition-B," 18<sup>th</sup> JANNAF Propulsion Systems Hazards Subcommittee Meeting, CPIA Publication 690, 1999.
4. Birk, A., Kooker, D.E. and Baker, P.J. "Model of Cavity Combustion Within an Energetic Solid:

Application to Composition-B," 19<sup>th</sup> JANNAF Propulsion Systems Hazards Subcommittee Meeting, CPIA Publication 704, 2000.

5. Lieb, R.J. and Baker, P.J. "Combustion Morphology of TNT and Composition-B," 19<sup>th</sup> JANNAF Propulsion Systems Hazards Subcommittee Meeting, CPIA Publication 704, 2000.
6. Baker, P. J. and Delaney, J., "The Nondetonative Response of Confined TNT and Composition-B," 17<sup>th</sup> JANNAF Propulsion Systems Hazards Subcommittee Meeting, CPIA Publication, 1998.
7. Baker, P. J. and Delaney, J., "Experiments for Nondetonative Reactions of Confined Explosives," 18<sup>th</sup> JANNAF Propulsion Systems Hazards Subcommittee Meeting, CPIA Publication 690, 1999.
8. Baker, P., Stegall, S., Kooker, D., Slack, W., Boyd, W., and Delaney, J., "Response of Composition-B to Rapid Compression," 19<sup>th</sup> JANNAF Propulsion Systems Hazards Subcommittee, CPIA Publication 704, 2000.
9. Krzewinski, B., Stegall, S., Baker, P. and Kooker, D. "Nondetonative Reaction Experiments on Confined PBXN-109," 20<sup>th</sup> JANNAF Propulsion Systems Hazards Subcommittee, CPIA To be Published, 2002.
10. Birk, A., Lieb, R., Blake, O., and Kooker, D.E. "Deflagration Experiments with Composition-B," 20<sup>th</sup> JANNAF Propulsion Systems Hazards Subcommittee, CPIA To be Published, 2002.
11. Ginsberg, M.J. and Asay, B.W. "Commercial carbon composition resistors as dynamic stress gauges in difficult environments," Rev. Sci. Instrum. 62(9), 1991
12. Gough, P.S. "The XNOVAKTC Code," BRL-CR-627, U.S. Army Ballistic Research Laboratory, Aberdeen Proving Ground, MD, February 1990.
13. Miller, M. S. and Vanderhoff, J. A., "Burning Phenomena of Solid Propellants", Army Research Laboratory Technical Report, ARL-TR-2551, July 2001.
14. Kondrikov, B. N., Raikova, V. M., and Samsonov, B. S., "Kinetics of the Combustion of Nitro Compounds at High Pressures," Translated from Fizika Goreniya I Vzryva, Vol. 9, No. 1, pp. 84-90, Jan-Feb 1973.
15. Lieb, R. and Baker, P. J., "Combustion Morphology of TNT and Composition-B," 19<sup>th</sup> JANNAF Propulsion Systems Hazards Subcommittee Meeting, CPIA Publication 704, Nov 2000.